Functional analysis of the effects of propofol on tamoxifen-resistant breast cancer cells: Insights into transcriptional regulation

RUNYANG YIN[1*], JING GAO[2*], YANG LIU[3] and CHUNYAN GUO[1]

[1]Department of Anesthesiology, The Affiliated Hospital of Inner Mongolia Medical University, Hohhot, Inner Mongolia Autonomous Region 010050, P.R. China; [2]First Clinical Medical College, The Affiliated Hospital of Inner Mongolia Medical University, Hohhot, Inner Mongolia Autonomous Region 010050, P.R. China; [3]Department of Clinical Laboratory, The Affiliated Hospital of Inner Mongolia Medical University, Hohhot, Inner Mongolia Autonomous Region 010050, P.R. China

Received September 18, 2024; Accepted February 6, 2025

DOI: 10.3892/ol.2025.14940

Abstract. Although 70% of patients with estrogen receptor-positive breast cancer benefit from tamoxifen (TAM) therapy, the development of resistance to TAM leads to high rates of metastasis and a poor prognosis. Propofol, a commonly used anesthetic, can inhibit the occurrence and progression of breast cancer. In the present study, the effects of propofol on TAM-resistant (TR) breast cancer cells were evaluated. MCF7-TR cells were treated with or without propofol. Subsequently, cell cycle progression and the induction of apoptosis were detected by flow cytometry, whereas cell proliferation was assessed using Cell Counting Kit-8 and colony formation assays. Furthermore, the potential transcriptional regulatory effects of propofol on MCF7-TR cells were investigated using RNA sequencing. The results indicated that propofol significantly promoted cell cycle arrest, induced apoptosis, and inhibited proliferation and colony formation in MCF7-TR cells. Furthermore, transcriptome sequencing analysis revealed 1,065 differentially expressed genes between propofol-treated MCF7-TR and untreated MCF7-TR cells. Gene Ontology annotation enrichment analysis, Kyoto Encyclopedia of Genes and Genomes pathway enrichment analysis and Gene Set Enrichment Analysis indicated that propofol affected the expression levels of genes located on the 'plasma membrane' and 'cell periphery', while mainly regulating signals involved in cancer biology, immune response and metabolic pathways. These results identified the potential effects of propofol on TR breast cancer cells and provided a theoretical basis for clinical treatment, particularly for individuals with TAM resistance.

Correspondence to: Dr Chunyan Guo, Department of Anesthesiology, The Affiliated Hospital of Inner Mongolia Medical University, 1 North Passage Road, Huimin District, Hohhot, Inner Mongolia Autonomous Region 010050, P.R. China
E-mail: 20060206@immu.edu.cn

Dr Yang Liu, Department of Clinical Laboratory, The Affiliated Hospital of Inner Mongolia Medical University, 1 North Passage Road, Huimin, Hohhot, Inner Mongolia Autonomous Region 010050, P.R. China
E-mail: liuyang@immu.edu.cn

*Contributed equally

Abbreviations: CDK, cyclin-dependent kinase; DEG, differentially expressed gene; ER, estrogen receptor; GO, Gene Ontology; GSEA, Gene Set Enrichment Analysis; KEGG, Kyoto Encyclopedia of Genes and Genomes; PCA, principal component analysis

Key words: propofol, tamoxifen resistance, breast cancer, RNA sequencing

Introduction

Breast cancer is a highly prevalent malignancy among women, which poses a threat to women's health, accounting for >23.8% of newly diagnosed cancer cases globally and for ~15.4% of cancer-related mortalities (1). In recent years, the global incidence and mortality rates of female breast cancer have shown an increasing trend each year, and its onset has been noted to occur more frequently in younger individuals (1,2). Common treatment approaches for breast cancer include surgery followed by chemotherapy or radiotherapy, targeted therapy and immunotherapy, as well as endocrine therapy. Tamoxifen (TAM), as a potent selective estrogen receptor (ER) modulator, has been reported to competitively bind to the ER on tumor cells, thereby preventing the action of estrogen on tumor cell proliferation (3). However, TAM resistance remains a notable obstacle that can lead to tumor relapse and metastasis in the majority of patients with breast cancer. Currently, there is no effective method to reverse TAM resistance in the clinic (4,5). Therefore, the identification of novel, non-toxic, broad-spectrum and cost-effective alternative agents to overcome TAM resistance is crucial in the prevention and treatment of breast cancer.

Propofol is a short-acting anesthetic used to induce sedation during a variety of surgical procedures (6). Recently, it has been shown to reduce cell viability, and inhibit the migratory and invasive abilities of breast cancer cells (7). In addition,

propofol has been reported to improve the overall survival (OS) and loco-regional recurrence-free survival (LRRFS) of patients with non-metastatic breast cancer, compared with inhalational anesthesia (8). Furthermore, a previous study demonstrated that propofol can enhance the sensitivity of patients with breast cancer to trastuzumab, reducing the local recurrence rate of patients undergoing breast-conserving surgery (9). These studies have suggested that propofol may be a promising candidate drug with important bioactivities that can be used as a therapeutic strategy against breast cancer. However, the potential regulatory effects of propofol on TAM-resistant (TR) breast cancer have not yet been determined.

Based on RNA sequencing (RNAseq) analysis, novel mechanisms of cancer progression and metastasis, involving numerous molecular and signaling pathways, have been demonstrated (10). For example, researchers have used RNAseq analysis to reveal aberrantly activated signaling pathways in the development of clear cell renal cell carcinoma and to uncover the oncogenic signaling pathways in patients with acral melanoma (11,12). Accumulating transcriptome sequencing data have suggested that the progression of tumorigenesis (such as cell cycle progression/arrest and suppression of apoptosis), immune response and metabolic regulation serve essential roles in the process of drug resistance in breast cancer (13-15). The progress in transcriptome sequencing has enabled its wider use in identifying targets of antitumor agents against multiple types of cancer (16,17).

The present study aimed to explore the potential regulatory mechanisms underlying the effects of propofol on TR breast cancer cells. The primary objectives were to detect the functions of propofol and to uncover the key singling pathways associated with propofol treatment in MCF7-TR cells. To achieve these aims, the current study employed a multi-faceted approach that included *in vitro* apoptosis and cell cycle analyses, proliferation and colony formation assays, and RNAseq analysis. By combining these methods, the study aimed to provide a comprehensive understanding of the effects of propofol on TR breast cancer, and to establish a foundation for the development of novel therapeutic targets for the treatment of TR breast cancer.

Materials and methods

Materials. Propofol (cat. no. HY-B0649) and TAM (cat. no. HY-13757A) were purchased from MedChemExpress. For the experiments, propofol and TAM were dissolved in dimethyl sulfoxide (DMSO) and further diluted in culture medium for storage. Cell Counting Kit-8 (CCK-8) (cat. no. P-CA-001) and phenol red-free high-glucose Dulbecco's Modified Eagle Medium (DMEM) (cat. no. PM150223) were purchased from Wuhan Pricella Biotechnology Co., Ltd. Certified charcoal-stripped fetal bovine serum (FBS; cat. no. 04-201-1A) was purchased from Biological Industries; Sartorius AG.

Cells. The human breast adenocarcinoma cell line MCF7 was purchased from American Type Culture Collection (cat. no. HTB-22). The cells were grown in complete DMEM supplemented with 10% charcoal-stripped FBS, penicillin (100 U/ml) and streptomycin (100 μg/ml) under standard conditions at 37˚C with 5% CO_2. MCF7-TR cells were prepared as described in previous reports with slight modifications (18,19). Briefly, the induction of TAM resistance was performed using culture medium containing 10 nM TAM for 48 h. Subsequently, the drug was removed and the cells underwent routine culturing, while continuously eliminating susceptible non-viable cells. Once the cell confluence reached 70-80%, the operation was repeated twice in succession. The selection process entailed iterative cycles, each time increasing the drug concentration incrementally. Specifically, the dosage of the drug was doubled with each iteration. This step-by-step adjustment continued until the cells could proliferate stably in a selection culture medium supplemented with 1 μM TAM. The parental control cells were treated with DMSO and underwent identical processing procedures as previously described (18,19). This entire process lasted ~12 months. To maintain TAM resistance, a concentration of 1 μM TAM was continuously supplemented to the MCF7-TR cell culture medium. In addition, the expression levels of two commonly studied TR-associated genes: ER 1 (*ESR1*) and ATP binding cassette subfamily B member 1 (*ABCB1*; also called P-glycoprotein), were detected in MCF7 and MCF7-TR breast cancer cells by reverse transcription-quantitative PCR (RT-qPCR). As shown in Fig. S1A, the expression of *ESR1* was downregulated, whereas *ABCB1* was upregulated in MCF7-TR cells as compared with in non-resistant parental MCF7 controls, which confirmed the successful construction of TAM resistance (20,21).

Total RNA extraction and RT-qPCR. RT-qPCR was conducted as described in a previous study (22). Briefly, MCF7-TR cells and parental non-resistant control cells were lysed in 1 ml TRIzol® (Invitrogen; Thermo Fisher Scientific, Inc.) on ice for 15 min. Subsequently, 200 μl chloroform was added to each sample to fully dissociate the nucleoprotein complex. Following centrifugation (12,000 x g, at 4˚C for 15 min), the upper aqueous phase was transferred to a new microcentrifuge tube and mixed with an additional 500 μl isopropyl alcohol to precipitate the RNA. After further centrifugation (12,000 x g, at 4˚C for 10 min), the RNA pellet was washed twice with 1 ml 75% ethanol. After air-drying, the RNA samples were resuspended in 100 μl diethyl pyrocarbonate-treated deionized water, and their concentrations were determined using a microspectrophotometer (NanoDrop 2000; Thermo Fisher Scientific, Inc.). For RT, first-strand cDNA was synthesized using the RevertAid First Strand cDNA Synthesis Kit (cat. no. K1622; Thermo Fisher Scientific, Inc.) according to the manufacturer's instructions. Subsequently, qPCR was carried out on a Bio-Rad CFX-Touch real-time PCR system (Bio-Rad Laboratories, Inc.) using the PowerTrack™ SYBR Green Master Mix (cat. no. A46012; Thermo Fisher Scientific, Inc.) according to the manufacturer's instructions. The thermocycling conditions were as follows: 95˚C for 30 sec for cDNA pre-denaturation; 95˚C for 10 sec for cDNA denaturation; 60˚C for 30 sec for primer annealing and new strand extension. With the exception of the pre-denaturation step, the denaturation, annealing and extension steps were repeated for a total of 40 cycles. *GAPDH* was used as a housekeeping gene. The primer sequences are listed in Table SI.

Cell cycle analysis and apoptosis detection. Cell cycle progression and the induction of apoptosis were analyzed using a Gallios flow cytometer (Beckman Coulter, Inc.) according to the manufacturer's instructions.

For cell cycle analysis, MCF7-TR cells were seeded in a 12-well plate at a density of $8x10^4$ cells/well and were incubated overnight. The cells were treated with 20 μM propofol for 24 h at 37˚C in an incubator with 5% CO_2, whereas the control cells were treated with an equal volume of DMSO. Subsequently, the cells were collected and centrifuged at 300 x g at 4˚C for 5 min. The cells were fixed with ice-cold 70% ethanol for 15 min on ice, washed with PBS, incubated with PI staining solution containing 50 μg/ml PI, 0.1 mg/ml RNase A and 0.05% Triton X-100 at room temperature for 1 h, and detected using a flow cytometer. The data were processed using the cell cycle fitting software ModFit LT 5.0 (Verity Software House, Inc.).

For apoptosis analysis, MCF7-TR cells were seeded in a 12-well plate at a density of $8x10^4$ cells/well and were incubated overnight. The cells were treated with 10 or 20 μM propofol for 24 h at 37˚C in an incubator with 5% CO_2, and the control cells were treated with an equal volume of DMSO. Subsequently, the cells were collected and centrifuged at 300 x g at 4˚C for 5 min. Apoptosis detection was performed using a fluorescein isothiocyanate Annexin V/PI kit (Becton, Dickinson and Company) according to the manufacturer's instructions. The samples were analyzed by fluorescence-activated cell sorting using a flow cytometer within 1 h of staining. The data were analyzed using Kaluza v. 1.2 (Beckman Coulter, Inc.), and the percentages of early apoptotic cells (Annexin V^+ and PI^-) and late apoptotic cells (Annexin V^+ and PI^+) were calculated.

Cell proliferation assay. Cell proliferation was assessed using the CCK-8 assay according to the manufacturer's instructions. Briefly, MCF7-TR cells and their parental cells were seeded at a density of $6x10^3$ cells/well and were cultured in 96-well plates overnight. Subsequently, 2.5 , 5 or 10 μM propofol was added to the cells and incubated for 0, 24, 48, 72 or 96 h. A total of 10 μl CCK-8 solution was then added to each well and incubated for 1 h. The absorbance value was detected at 450 nm using a spectrophotometer (Synergy HT; BioTek; Agilent Technologies, Inc.).

Colony formation assay. The colony formation assay was performed as described in a previous study (23). Briefly, MCF7-TR cells were seeded in 6-well plates at a density of $1x10^3$ cells/well and were cultured overnight. Subsequently, 2.5 μM propofol was added to each well and the control cells were treated with an equal volume of DMSO Subsequently, the medium was replaced with fresh complete medium on day 3. On day 6, the cell colonies were fixed with 4% paraformaldehyde (cat. no. P0099; Beyotime Institute of Biotechnology) for 10 min at room temperature. After being washed twice with distilled water for 2 min each time, the colonies were stained with 2 ml/well crystal violet solution (cat. no. C0121; Beyotime Institute of Biotechnology) for 10 min at room temperature. After washing twice with distilled water (5 min/wash), the plates were scanned using a scanner (HP ScanJet Pro 2600 f1; HP Development Company, L.P.) and the colonies were calculated manually using an inverted light microscope (CKX53; Olympus Corporation). Colonies with cell numbers >20 were counted.

Total RNA extraction, library construction and sequencing. A total of $5x10^6$ MCF7-TR cells were seeded in a 6-cm cell culture dish and cultured overnight. Subsequently, propofol (10 μM) was added to each plate and the cells were cultured for 24 h. The control cells were treated with an equal volume of DMSO. Total RNA was obtained from propofol-treated or non-treated MCF7-TR cells using TRIzol reagent according to the manufacturer's instructions. The quality and concentration of mRNA were detected using a NanoDrop 2000 spectrophotometer (Thermo Fisher Scientific, Inc.). The purified mRNA from three repeat samples of the solvent control and propofol-treated MCF7-TR cells was processed to prepare an mRNAseq library using Illumina Stranded Total RNA Prep with Ribo-Zero Plus or Ribo-Zero Plus Microbiome kit (Illumina, Inc.) (24). Briefly, ribosomal RNAs were eliminated by a poly-(A) containing mRNA selection procedure to minimize their sequencing. Subsequently, the remaining mRNAs were subjected to cDNA strand synthesis, purification, end-repair, A-tailing adaptor ligation and PCR amplification. The library quality was analyzed using Agilent Bioanalyzer 2100 (Agilent Technologies, Inc.) and the concentrations of the libraries were detected by qPCR analysis. Subsequently, 20 pM each library was sequenced using an Illumina NextSeq500 instrument (Illumina, Inc.) equipped with NextSeq System Suite v2.2.0 software (Illumina, Inc.). Paired-end reads with a length of 150 bp were harvested using the NextSeq 550 System High-Output Sequencing Kit (Illumina, Inc.).

Functional and signaling pathway enrichment analysis of differentially expressed genes (DEGs). Differential gene expression analysis and principal component analysis (PCA) were conducted using the DESeq package (https://bioconductor.org/packages//2.10/bioc/html/DESeq.html) and depicted using the FactoMineR package (https://cran.r-project.org/web/packages/FactoMineR/index.html) in R (version 4.4.2; https://www.r-project.org/). Genes with |log2FoldChange|>1 and P<0.05 were identified as being differentially expressed. Two-way cluster analysis on all DEGs was performed using the pheatmap package (https://cran.r-project.org/web/packages/pheatmap/index.html), based on expression levels across samples and patterns within samples, using Euclidean distance and complete linkage hierarchical clustering. Volcano plots were generated using the ggplot2 package (https://cran.r-project.org/web/packages/ggplot2/index.html). Data analysis for gene expression was performed based on the Database for Annotation, Visualization and Integrated Discovery (https://davidbioinformatics.nih.gov/). DEGs underwent GO enrichment analysis to determine the enriched biological processes, cellular components and molecular functions (http://www.geneontology.org/). The signaling pathways were investigated using the Kyoto Encyclopedia of Genes and Genomes (KEGG) pathway (http://www.genome.jp/kegg/). In addition, Gene Set Enrichment Analysis (GSEA) was performed using GSEA software (https://www.broadinstitute.org/gsea/) using the following: Permutation, geneset; metric, Diff_of_classes; metric, weighted; # permutation, 2,500.

Statistical analysis. Data are presented as the mean ± SD and are representative of three independent experiments. Data analysis was performed using GraphPad Prism 7 (Dotmatics).

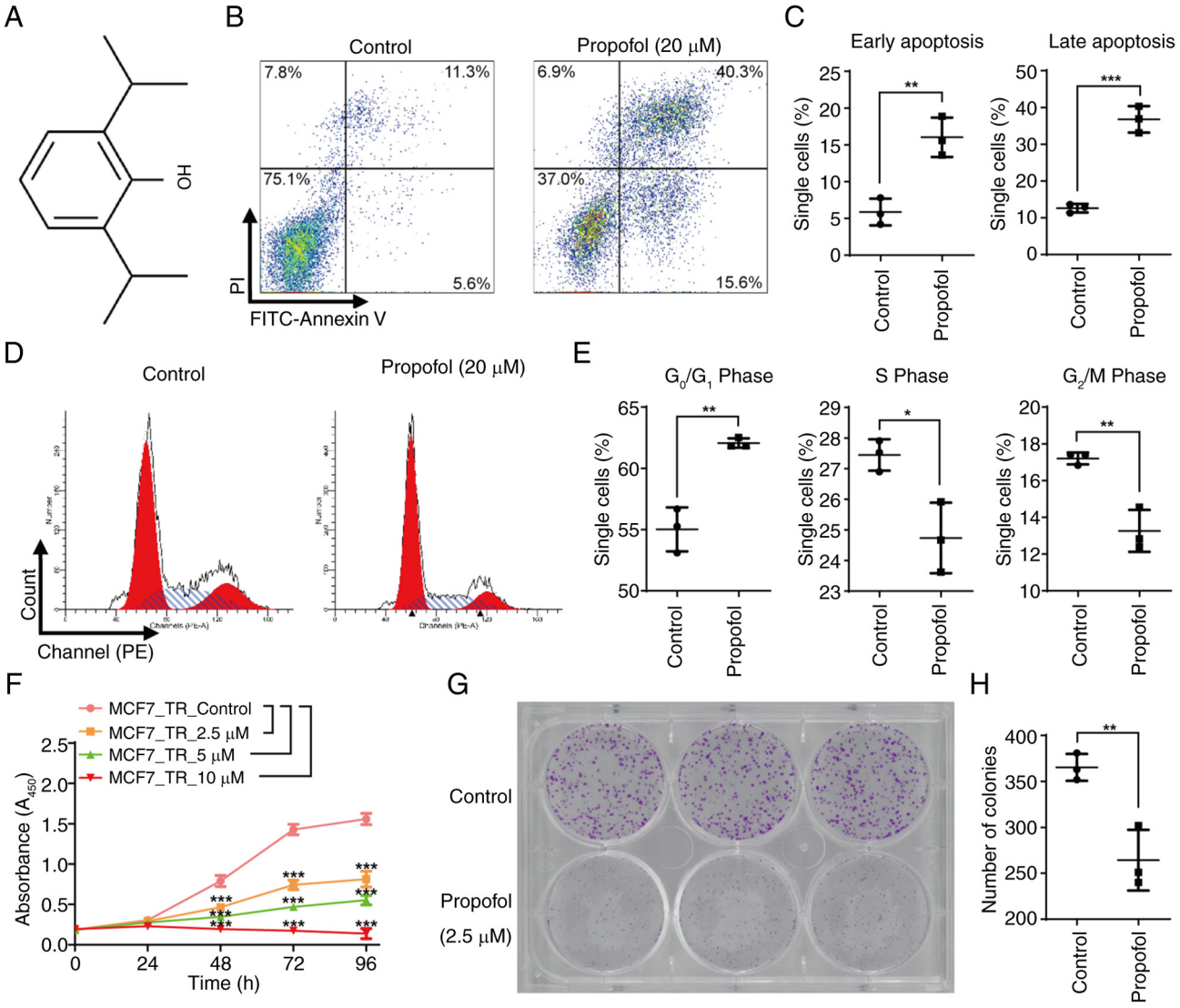

Figure 1. Propofol significantly promotes apoptosis and cell cycle arrest, and inhibits proliferation and colony formation in MCF7-TR cells. (A) Chemical structure of propofol. (B) Propofol significantly promoted the apoptosis of MCF7-TR cells. MCF7-TR cells were treated with or without propofol (20 μM) for 24 h, stained with PI and Annexin V, and apoptosis was detected using flow cytometry. (C) Percentage of Annexin V^+ and PI^- early apoptotic cells, and Annexin V^+ and PI^+ late apoptotic cells. (D) Propofol significantly promoted the cell cycle arrest of MCF7-TR cells. MCF7-TR cells were treated with or without propofol (20 μM) for 24 h, stained with PI and cell cycle progression was detected using flow cytometry. (E) Percentage of cells in G_0/G_1, S and G_2/M phases. (F) Propofol significantly inhibited the proliferation in MCF7-TR cells. MCF7-TR cells were treated with 2.5, 5 and 10 μM propofol for 24, 48, 72 and 96 h, and were incubated with 10 μl Cell Counting Kit-8 for 1 h before absorbance was measured using a spectrophotometer. (G) Propofol significantly inhibited colony formation in MCF7-TR cells. MCF7-TR cells were treated with or without propofol (2.5 μM) for 6 days, stained with crystal violet and images were captured using a scanner. (H) Number of colonies in propofol-treated and untreated MCF7-TR cells. Data are presented as the mean ± SD. Significant differences were examined using a (C, E and H) two-tailed Student's t-test or (F) a two-way analysis of variance. *P<0.05, **P<0.01, ***P<0.001. TR, tamoxifen-resistant.

Statistical significance between two experimental groups was evaluated using an unpaired two-tailed Student's t-test. Multiple sets of data were compared using a one- or two-way analysis of variance with Tukey's post hoc test. P<0.05 was considered to indicate a statistically significant difference.

Results

Propofol treatment significantly promotes apoptosis and cell cycle arrest and inhibits proliferation and colony formation in MCF7-TR cells. Fig. 1A shows the chemical structure of propofol. To investigate the effect of propofol on MCF7-TR cells, the cells were incubated with 10 and 20 μM propofol for 24 h. Apoptosis induction was then analyzed by flow cytometry (Figs. 1B, 1C, S1B and S1C). Notably, 10 μM propofol caused only a slight, but significant, increase in both early and late apoptosis of MCF7-TR cells (Fig. S1C), whereas 20 μM resulted in a significant increase (Figs. 1C and S1C). Therefore, 20 μM propofol was selected for further analysis. Propofol at a concentration of 20 μM induced a marked increase in the percentage of MCF7-TR cells present in the G_0/G_1 phase, and notable decreases in the percentage of cells present in the S and G_2/M phases of the cell cycle compared with in the control group, suggesting that it induced significant cell cycle arrest (Fig. 1D and E). Considering that 20 μM propofol may induce significant apoptosis and cell cycle arrest, lower concentrations of propofol, specifically 2.5, 5 and 10 μM, were selected for the cell proliferation assay. Consistent with these findings,

propofol treatment markedly inhibited cell proliferation in a dose-dependent manner. Notably, when the concentration of propofol reached 10 μM, it caused a significant decrease in the proliferation of MCF7-TR cells after 96 h of incubation (Fig. 1F). MCF7-TR cells exhibited greater sensitivity to propofol compared with non-TR control cells, as evidenced by significantly reduced cell proliferation in MCF7-TR cells following propofol treatment (Fig. S1D). Since prolonged exposure to either 5 or 10 μM propofol significantly reduced cell proliferation (Fig. 1F), a concentration of 2.5 μM was selected to investigate its effects on cell colony formation. In the cells treated with 2.5 μM propofol, both the size and number of colonies were markedly reduced compared with in the cells treated with a solvent control, indicating that propofol exerted an inhibitory effect on the colony-forming ability of MCF7-TR cells (Fig. 1G and H). These results indicated that propofol exhibited potential antitumor characteristics in TR breast cancer cells.

Propofol treatment affects MCF7-TR gene expression profiles. RNAseq analysis was performed for MCF7-TR cells treated with or without propofol. Given that a 24-h treatment with 20 μM propofol resulted in a significant increase in the apoptosis of MCF7-TR cells (Figs. 1B, 1C, S1B and S1C), 10 μM propofol was selected to investigate its gene regulatory effects on MCF7-TR cells. PCA indicated optimal intergroup difference and intragroup consistency between MCF7-TR cells treated with or without propofol (Fig. 2A). A total of 1,065 DEGs were identified in MCF7-TR cells following treatment with propofol, in which the expression levels of 685 genes were markedly downregulated and those of 380 genes were upregulated compared with those in the control cells (Fig. 2B-D; Table SII). Overall, propofol treatment markedly altered the gene expression profiles of MCF7-TR cells.

GO term classification and KEGG pathway enrichment analysis. In order to identify the key biological processes in which the DEGs in propofol-treated MCF7-TR cells were involved, the molecular functions they exerted and the pivotal signaling pathways they were involved in, GO term classification and KEGG enrichment analysis were performed. As shown in Fig. 3A, a high number of DEGs in MCF7-TR cells treated with propofol were clustered in the 'cell periphery' and located in the 'plasma membrane', possessing phosphatase activity, and were involved in the regulation of the immune response and in the phosphorylation processes. Furthermore, KEGG enrichment analysis indicated that various enriched pathways in all treated cells were related to the process of 'transcriptional misregulation in cancer' and 'cell cycle', which occur in cancer biology (Fig. 3B). In addition, the enriched signaling pathways that were identified were associated with specific immune response processes, as indicated by 'cytokine-cytokine receptor interaction' and 'chemokine signaling pathway', and the endocrine system, as indicated by 'estrogen signaling pathway' and 'progesterone-mediated oocyte maturation' according to the rich-factor and false discovery rate (FDR) values (Fig. 3B). These results indicated that propofol treatment could markedly regulate tumor biology-associated processes, immune response and metabolism.

Propofol treatment affects gene expression profiles in the immune response process in MCF7-TR cells. Based on the GO term classification and the KEGG enrichment analysis, the DEGs involved in immune response-associated signaling pathways were further analyzed. As shown in Fig. 4, the top four most dysregulated signaling pathways, according to the rich factor and FDR value, in MCF7-TR cells treated with propofol were as follows: Chemokine signaling pathway (Fig. 4A), IL-17 signaling pathway (Fig. 4B), TNF signaling pathway (Fig. 4C) and leukocyte transendothelial migration (Fig. 4D). Among these pathways, DEGs affected by propofol treatment were mainly clustered into the chemokine signaling pathway, in which 13 genes were upregulated and seven genes were markedly downregulated (Fig. 4A). In addition, for TNF signaling pathway, two genes (MMP9 and TRAF1) were significantly downregulated, and seven genes were upregulated upon propofol administration (Fig. 4C). These results suggested that propofol administration in MCF7-TR cells significantly regulated immune response signals, mainly manifested by the chemokine signaling pathway.

Propofol treatment affects the gene expression profiles associated with the metabolic process in MCF7-TR cells. The enriched DEGs involved in the metabolic process, according to the rich factor and FDR value, were analyzed and are shown in Fig. 5. The impact of propofol on metabolism was characterized by riboflavin metabolism (Fig. 5A), fatty acid biosynthesis (Fig. 5B), thyroid hormone synthesis (Fig. 5C) and arachidonic acid metabolism (Fig. 5D). Among these processes, the effect of propofol on metabolic regulation was mainly characterized by inhibition of the expression levels of metabolism-related genes. No upregulated genes were noted in the processes of riboflavin metabolism and fatty acid biosynthesis, and higher numbers of downregulated genes were noted in the thyroid hormone synthesis and arachidonic acid metabolism processes in MCF7-TR cells following treatment with propofol compared with in the control cells. These findings indicated that propofol was involved in regulation of the metabolic process, which was mainly dependent on downregulation of the expression levels of metabolic genes.

Signaling pathways involved in the sensitivity of MCF7-TR cells to propofol. To further characterize the molecular functions involved in the immune response and metabolism, based on the findings from the GO and KEGG analyses in propofol-treated MCF7-TR cells, GSEA was performed on the RNAseq data (Fig. 6). The negatively enriched gene sets were involved in ABC transporters (Fig. 6A), the adipocytokine signaling pathway (Fig. 6B), and aldosterone synthesis and secretion (Fig. 6C), while the positively enriched gene set was involved in the aminoacyl-tRNA biosynthesis (Fig. 6D). These gene sets were composed of genes associated with certain metabolites, which indicated that propofol functions partially by activating and inhibiting metabolism-related signaling pathways.

Discussion

Currently, breast cancer is the leading cause of morbidity and mortality among women. Among all types of breast

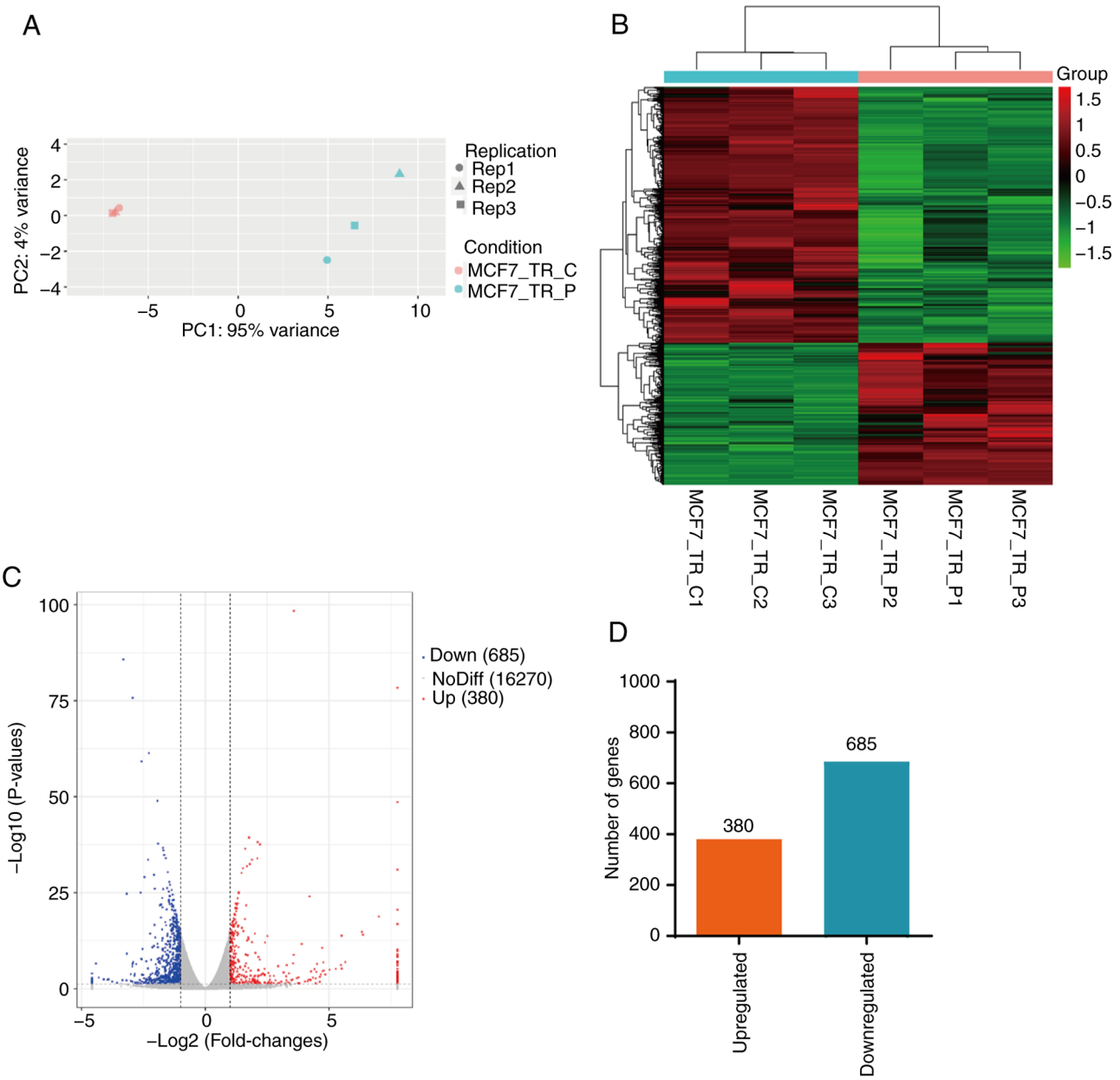

Figure 2. Propofol regulates MCF7-TR cell gene expression profiles. MCF7-TR cells were treated with or without 10 μM propofol for 24 h. The mRNA expression levels were detected by RNA sequencing. (A) PC analysis was performed using the DESeq package and depicted using the FactoMineR package in R software to show inter-group differences and intra-group consistency. (B) Heat map indicating the DEGs between propofol-treated and untreated MCF7-TR cells. Two-way cluster analysis of all DEGs was carried out using the pheatmap package. The clustering was performed based on the expression level of the same gene in different samples and the expression patterns of different genes in the same sample. (C) Volcano plot indicating DEGs between propofol-treated and untreated MCF7-TR cells. The volcano plot of DEGs was drawn using the ggplot2 package in R software. The two vertical dotted lines represent the threshold of 2-fold change expression difference and the horizontal dotted line represents the P=0.05 threshold. The red dots indicate upregulated genes, the blue dots indicate downregulated genes and the gray dots indicate genes with no significant difference in expression. (D) Number of DEGs that were significantly upregulated and downregulated between propofol-treated and untreated MCF7-TR cells. The criteria for identifying DEGs were: |log2FoldChange|>1 and P<0.05. MCF7_TR_C1, MCF7_TR_C2 and MCF7_TR_C3 represent the control samples; and MCF7_TR_P1, MCF7_TR_P2 and MCF7_TR_P3 represent MCF7-TR cells treated with 10 μM propofol. DEGs, differentially expressed genes; PC, principal component; rep, replication; TR, tamoxifen-resistant.

cancer, ER$^+$ breast cancer is the most common, and the ER signaling pathway serves a key role in its occurrence and development (25). Therefore, endocrine therapy that blocks the effects of estrogen has become the first-line treatment for patients with ER$^+$ breast cancer (26). However, the primary and acquired resistance encountered by patients receiving endocrine drugs, such as TAM, remains an unsolved clinical challenge. The present study demonstrated that propofol can affect cell cycle progression and induce the apoptosis of TR breast cancer cell lines by altering gene expression profiles involved in the regulation of tumorigenesis, immune response and metabolism.

Numerous studies have suggested that the development, metastasis and recurrence of tumors are closely related to the cell cycle, apoptosis and proliferation, and disruption of these events have been confirmed to be the fundamental hallmarks of human malignancies (27-29). Notably, misregulation in the cell cycle-related signaling pathways can result

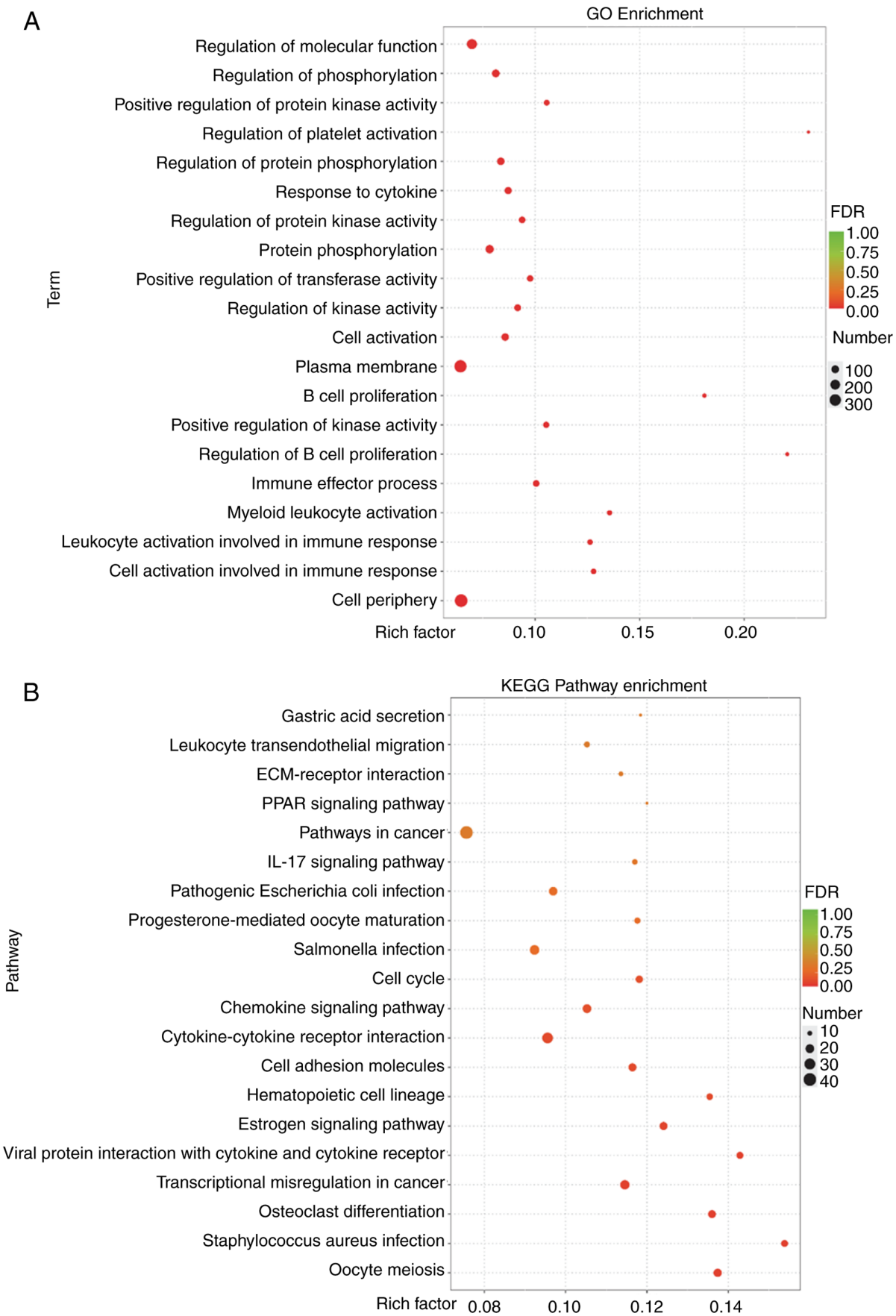

Figure 3. GO term classification and KEGG pathway enrichment analysis. (A) Scatter plot of the top 20 most significantly enriched GO terms (biological processes, cellular components and molecular functions) of differentially expressed genes in MCF7-TR cells following treatment with 10 μM propofol for 24 h. (B) Scatter plot of the top 20 most significantly enriched KEGG signaling pathways obtained from the RNA sequencing data from MCF7-TR cells following treatment with 10 μM propofol for 24 h. The degree of enrichment is indicated by rich factor, FDR and the number of genes. FDR, false discovery rate; GO, Gene Ontology; KEGG, Kyoto Encyclopedia of Genes and Genomes; TR, tamoxifen-resistant.

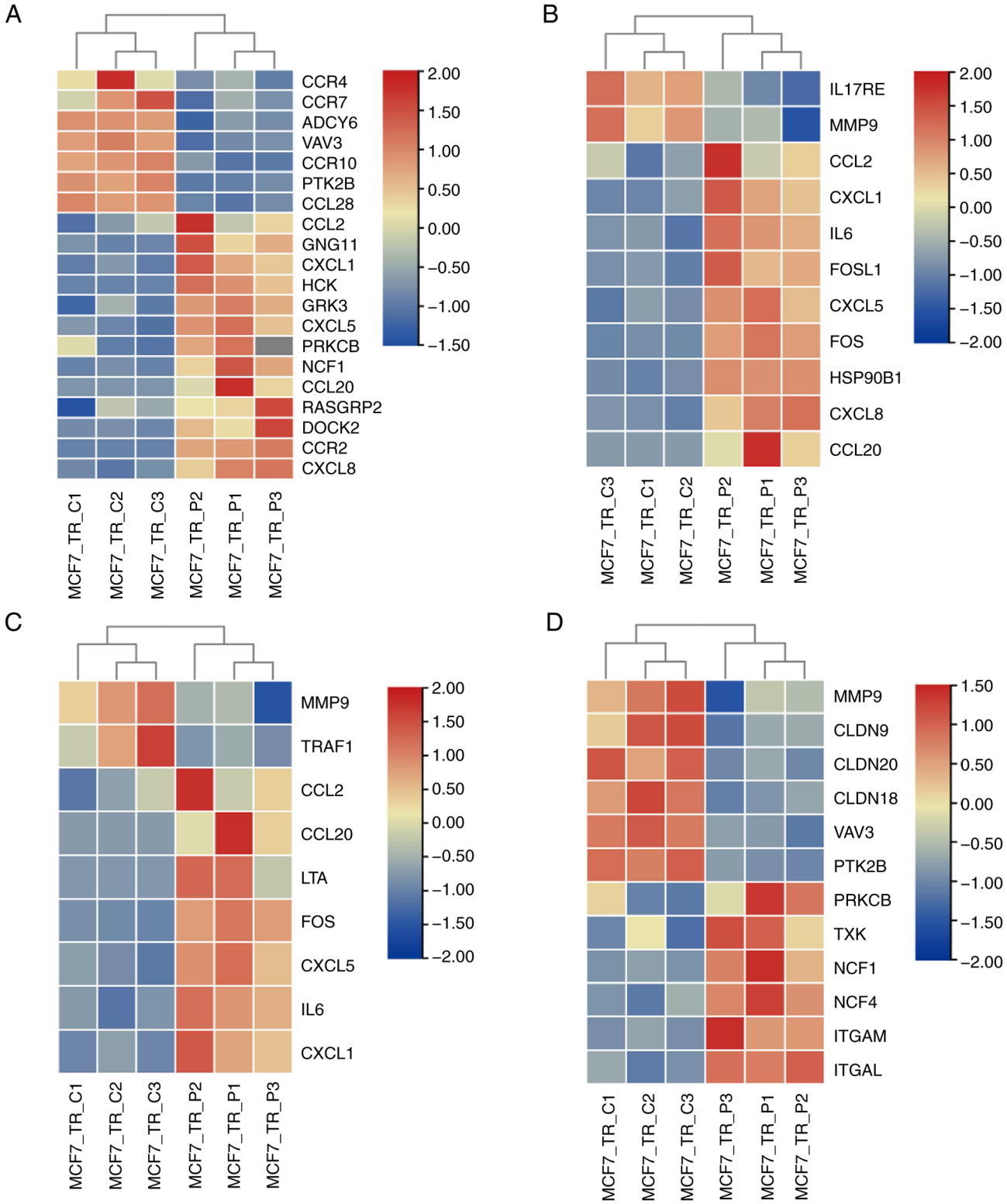

Figure 4. Propofol treatment affects gene expression profiles in the immune response process in MCF7-TR cells. MCF7-TR cells were treated with or without 10 μM propofol for 24 h. The mRNA expression levels were detected by RNA sequencing. Heat maps indicated that differentially expressed genes in MCF7-TR cells treated with propofol were involved in the (A) chemokine signaling pathway, (B) IL-17 signaling pathway, (C) TNF signaling pathway (D) and leukocyte transendothelial migration signaling pathway. MCF7_TR_C1, MCF7_TR_C2 and MCF7_TR_C3 represent the control samples; and MCF7_TR_P1, MCF7_TR_P2 and MCF7_TR_P3 represent MCF7-TR cells treated with 10 μM propofol. TR, tamoxifen-resistant.

in the unlimited proliferation of tumor cells. Moreover, it has been reported that one approach to enhance the sensitivity of cancer cells to chemotherapeutics can be achieved by combining them with cell cycle regulators (30). Preclinical studies have shown that propofol can significantly inhibit the development of breast cancer tumors by promoting apoptosis and arresting the cell cycle (7,31-33). Furthermore, TR breast cancer cells exhibit greater sensitivity to propofol compared

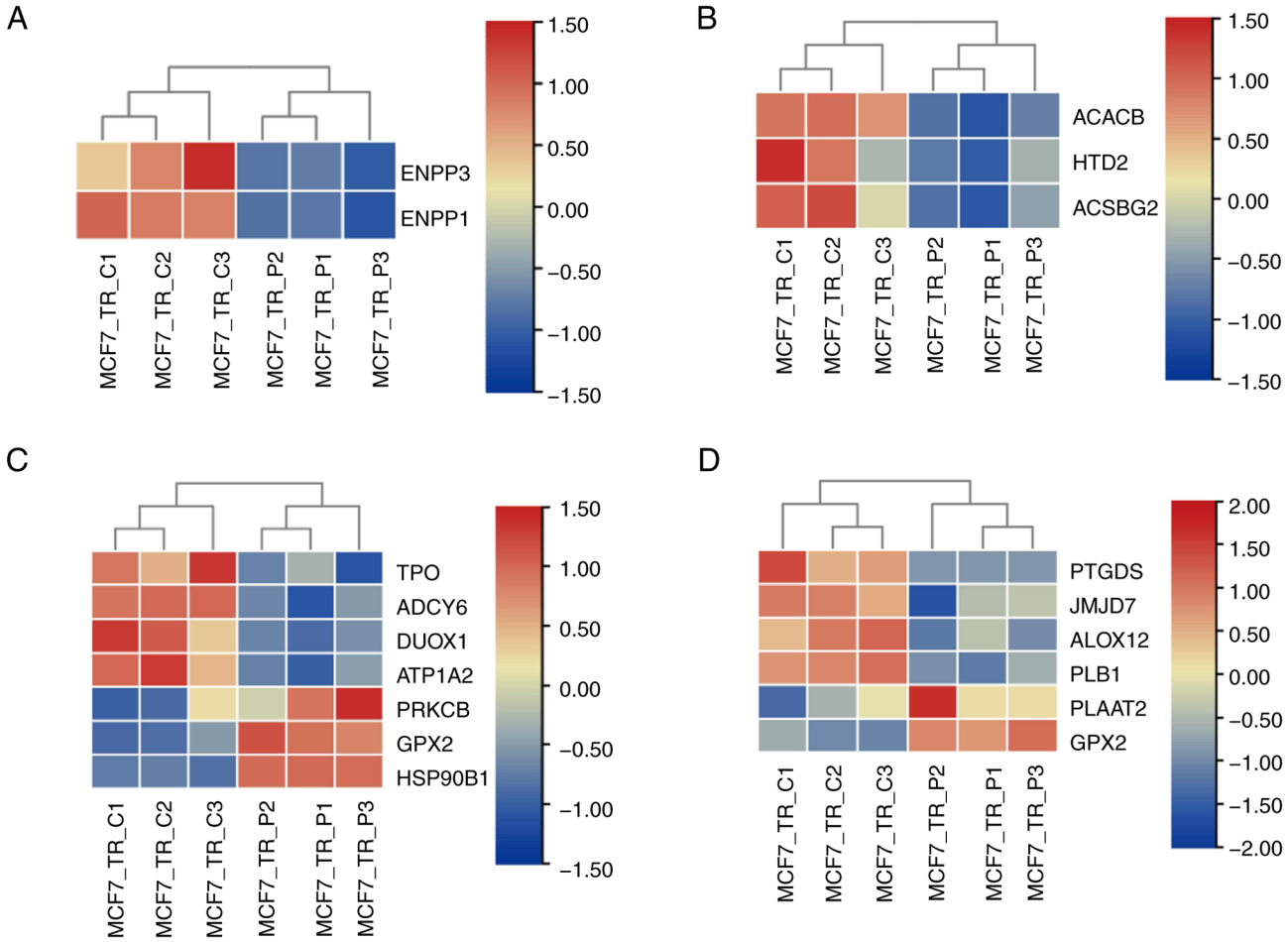

Figure 5. Propofol treatment affects gene expression profiles associated with the metabolic process in MCF7-TR cells. MCF7-TR cells were treated with or without 10 μM propofol for 24 h. The mRNA expression levels were detected by RNA sequencing. Heat maps indicated that differentially expressed genes in MCF7-TR cells treated with propofol were involved in the (A) riboflavin metabolism process, (B) fatty acid biosynthesis process, (C) thyroid hormone synthesis process and (D) arachidonic acid metabolism process. MCF7_TR_C1, MCF7_TR_C2 and MCF7_TR_C3 represent the control samples; and MCF7_TR_P1, MCF7_TR_P2 and MCF7_TR_P3 represent MCF7-TR cells treated with 10 μM propofol. TR, tamoxifen-resistant.

with non-TR breast cancer cells. For non-TR cells, a minimum of 25 μg/ml propofol (equivalent to 140 μM) is required to induce significant apoptosis (7), whereas in the present study, only 20 μM propofol was sufficient to achieve similar effects in TR breast cancer cells. Additionally, the study revealed that concentrations as low as 2.5 μM propofol could inhibit cell proliferation and colony formation in TR breast cancer cells. These concentrations are much lower than those used for clinical anesthesia induction (1.5-2.5 mg/kg body weight) and maintenance (4-12 mg/kg body weight/h) (34). This lower effective concentration is particularly important for patients with TR breast cancer, as it suggests a broader therapeutic window for propofol (35). In the clinical setting, the effects of propofol have been perplexing. A previous study has shown a lack of association between propofol-based total intravenous anesthesia and inhalation anesthesia and long-term survival following cancer surgery in Korean individuals (36). However, a broader meta-analysis (including four randomized clinical trials and 13 retrospective cohort studies) demonstrated that propofol-based anesthesia can significantly improve OS and LRRFS in patients with non-metastatic breast cancer, compared with inhalational anesthesia (8). In the present study, the antitumor activity of propofol was characterized by inhibited cell cycle progression, increased cell apoptosis and inhibited proliferation. These findings suggested that propofol may act as a cell cycle regulator in TR breast cancer cells and could be a potential effective drug for patients who are resistant to anti-endocrine therapy.

In accordance with the *in vitro* results, the data obtained from transcriptome sequencing analysis indicated that a large number of DEGs in MCF7-TR cells treated with propofol were enriched in the process of cell cycle and transcriptional misregulation. The cell cycle mainly consists of the following two key events: Interphase, and the mitotic or M phase. The transitions between the cell cycle phases are triggered by the cyclin-dependent kinases (CDKs) and their binding ligands in the cyclin protein family (37,38). CDK4/6 inhibitors have been employed as potent, selective and orally bioavailable treatments for hormone receptor-positive, $HER2^-$ breast cancer (39,40). In the present study, propofol administration resulted in a marked inhibition in the number of MCF7-TR cells in S phase of the cell cycle, implying a potential association with CDK4/6 signals. Preclinical studies have indicated that various cell cycle-associated proteins are implicated in the resistance of tumors to CDK4/6 inhibitors. For example, the dysregulation of the cell cycle specific proteins INK4,

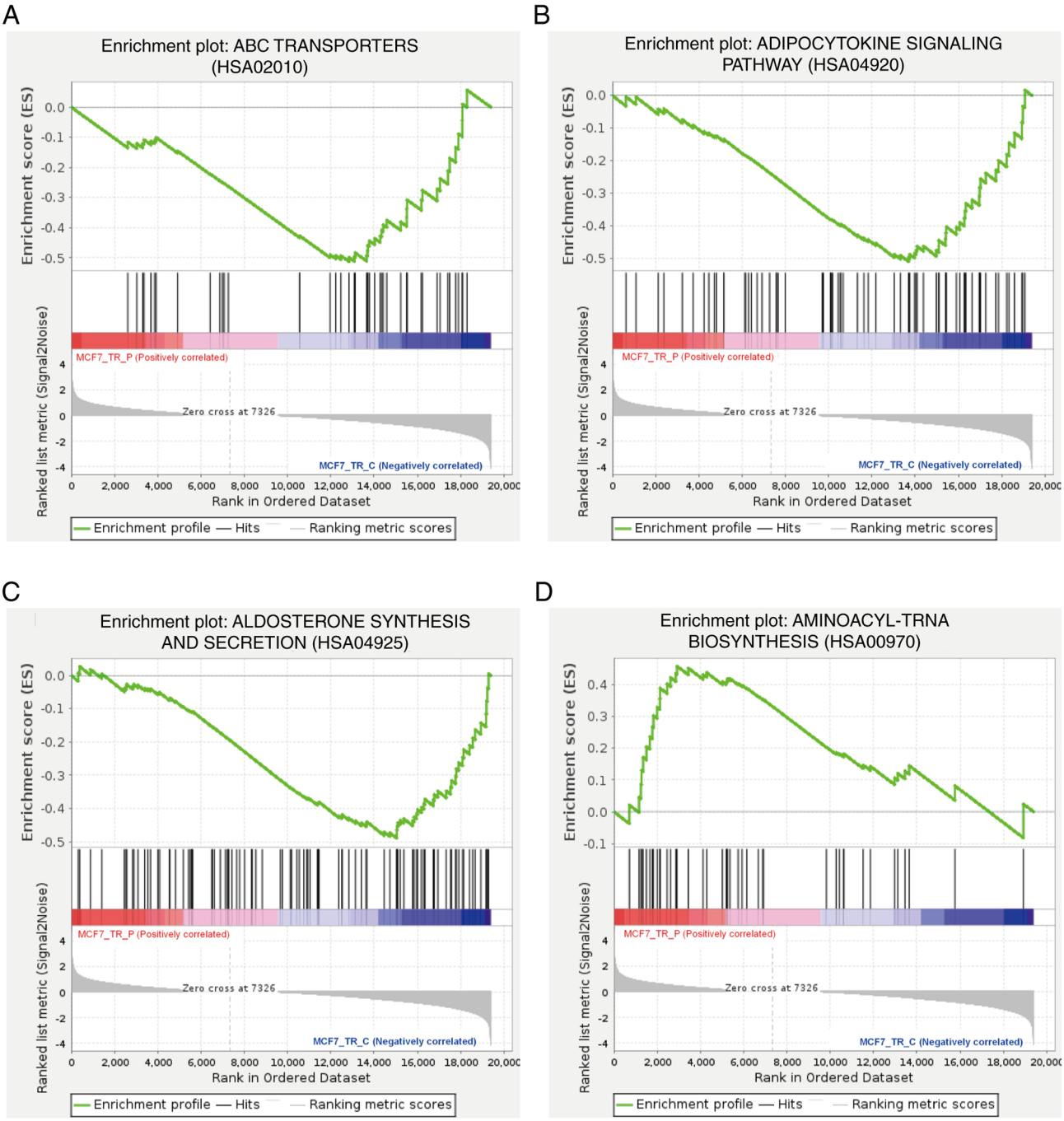

Figure 6. Signaling pathways involved in the sensitivity of MCF7-TR cells to propofol. MCF7-TR cells were treated with or without 10 μM propofol for 24 h. The mRNA expression levels were detected by RNA sequencing. Gene Set Enrichment Analysis plots indicated that differentially expressed genes in MCF7-TR cells treated with propofol were involved in the (A) ABC transporters pathway, (B) adipocytokine signaling pathway, (C) aldosterone synthesis and secretion, (D) and aminoacyl-tRNA biosynthesis. TR, tamoxifen-resistant.

Supplementary figure legend

p21 and P27 has been reported to mediate the resistance to CDK4/6 inhibitors in breast cancer (41-43). CDK4/6 inhibition and cytostasis evasion are two critical events that occur in ER$^+$ breast cancer cells, and combined targeting of both CDK4/6 and PI3K can induce cancer cell apoptosis *in vitro* and in patient-derived tumor xenograft models, and prevent resistance to CDK4/6 inhibitors by reducing the levels of cyclin D1 and other G_1-S cyclins, which ultimately results in tumor regression (44). The aforementioned studies indicate that the targets of propofol in TR breast cancer cells may also function as components of G_1-S cyclins, which require further exploration in future studies.

In addition to the DEGs enriched in the cell cycle involved in the regulation of tumor occurrence and recurrence, those affected by propofol treatment were also clustered into immune and metabolic signaling pathways. The results from KEGG pathway analysis indicated that certain DEGs were significantly enriched into the chemokine signaling pathway. A previous study has indicated that C-X-C motif ligand (CXCL)10, which is a pro-inflammatory

cytokine secreted by tumor cells, serves a vital role in TR in breast cancer (45). CXCL10 can promote breast cancer proliferation and growth via both estrogen-dependent and -independent pathways, whereas CXCL10 inhibition has been shown to reverse the resistance of cells to TAM (46). In addition, chemokines and their receptors, such as C-X3-C motif chemokine ligand 1, CXCL12 and C-X-C chemokine receptor type 4 have been identified as biomarkers for TR breast cancer therapy (47,48). Moreover, the present study indicated that ~40 DEGs contributed to regulation of the cytokine-cytokine receptor interaction, manifested by the activation of IL-17 and the TNF signaling pathway. TNF receptor-associated factor 1 (TRAF1) is a signaling adaptor known for its role in TNF receptor-induced cell survival, and serves a pivotal role in tumorigenesis and metastasis (49). The expression levels of TRAF1 have been reported to be significantly associated with a longer disease-free survival rate of breast cancer (50), and knockdown of TRAF1 expression may increase TAM sensitivity in breast cancer cells (51). In the present study, propofol downregulated TRAF1 levels, suggesting its potential for reversing TAM resistance in breast cancer, which requires further elucidation. In addition, the present study demonstrated that metabolic processes, such as riboflavin metabolism, fatty acid biosynthesis, thyroid hormone synthesis and arachidonic acid metabolism, were processes involved in the response of MCF7-TR cells to propofol; within these processes, the expression levels of the majority of the genes were downregulated. The results of the present study are supported by previous findings reported by Jiang *et al* (52); this previous study demonstrated that targeting fatty acid metabolism inhibition could overcome TAM resistance in ER^+ breast cancer. Furthermore, the results from the GSEA indicated that significant metabolites, including adipocytokines, aldosterone and aminoacyl-tRNA, were strongly associated with propofol sensitivity. These findings suggested that the activation and/or inhibition of the signaling pathways in which these metabolites are involved may have an important role in counteracting TAM resistance in breast cancer cells. Collectively, the present study elucidated a potential mechanism by which propofol regulates functions in TR breast cancer cells at the transcriptional level, providing valuable insights for the clinical application of this anesthetic drug, particularly in individuals who are resistant to TAM. Future investigations employing gene knockout and transgene experiments, as well as *in vivo* and *in vitro* studies, will be conducted to further explore the immune response and metabolic pathways implicated in the present study, aiming to identify the underlying mechanism for propofol-mediated regulation of TR breast cancer.

The present study revealed that a 24-h incubation with 20 μM propofol was sufficient to promote cell cycle arrest and trigger apoptosis, demonstrating its potential as a cell cycle regulator for the treatment of breast cancer. Although the impact of different propofol concentrations on the gene expression profile of cells remains unclear, cell phenotype assays suggested that a lower concentration with a longer duration (2.5 or 5 μM for 3-6 days) may regulate the expression of genes associated with cell proliferation. Conversely, a shorter culturing time with a higher concentration of propofol (10 or 20 μM for 24 h) may induce the expression of genes related to apoptosis, cell cycle arrest, inflammatory response and metabolic changes. As the results of the present study indicated lower effective concentrations of propofol on TR breast cancer cells, and identified several therapeutic genes and pathway targets of propofol in TR breast cancer cells, this work is anticipated to make notable contributions to the field of breast cancer treatment and may lead to more effective therapies for patients with TAM resistance. However, the present study was constrained by its exclusive focus on gene transcription in cell lines and the exclusion of potential regulatory mechanisms associated with protein expression levels. Future experiments will focus on investigating the DEGs and their associated signaling pathways. Gene knockout and transgenic mouse models, as well as cell lines, will be utilized to elucidate the mechanisms by which these DEGs and pathways confer resistance to TAM. Additionally, the synergistic effects of combining small molecule inhibitors targeting these DEGs and pathways with propofol will be explored to develop more effective therapeutic strategies. Clinically, it is also crucial to evaluate the potential benefits of the use of propofol for patients with TR breast cancer, which can significantly guide the selection of anesthetics in breast cancer surgery.

Acknowledgements

Not applicable.

Funding

This work was supported by a grant from the Scientific Research Project of Higher Education Institutions of Inner Mongolia Autonomous Region (grant no. NJZZ23016).

Availability of data and materials

The RNA sequencing data generated in the present study may be found in the NCBI BioProject database under accession number PRJNA1021154 or at the following URL: https://www.ncbi.nlm.nih.gov/bioproject/PRJNA1021154. The other data generated in the present study may be requested from the corresponding author.

Authors' contributions

RY, CG and YL conceptualized the study. RY and JG designed the study, and collected and analyzed the data. RY, JG, YL and CG wrote and edited the manuscript. CG provided the funding. CG and YL supervised the research. RY, YL and CG confirm the authenticity of all the raw data. All authors read and approved the final version of the manuscript.

Ethics approval and consent to participate

Not applicable.

Patient consent for publication

Not applicable.

Competing interests

The authors declare that they have no competing interests.

References

1. Bray F, Laversanne M, Sung H, Ferlay J, Siegel RL, Soerjomataram I and Jemal A: Global cancer statistics 2022: GLOBOCAN estimates of incidence and mortality worldwide for 36 cancers in 185 countries. CA Cancer J Clin 74: 229-263, 2024.
2. Siegel RL, Miller KD, Wagle NS and Jemal A: Cancer statistics, 2023. CA Cancer J Clin 73: 17-48, 2023.
3. Kim J and Munster PN: Estrogens and breast cancer. Ann Oncol 36: 134-148, 2025.
4. Chen F, Wang L, Feng Y, Ma W, Liu J, Bi Q, Song Y, Gao R and Jia Y: F-box and leucine-rich repeat protein 16 controls tamoxifen sensitivity via regulation of mitochondrial respiration in estrogen receptor-positive breast cancer cells. Hum Cell 36: 2087-2098, 2023.
5. Hanker AB, Sudhan DR and Arteaga CL: Overcoming endocrine resistance in breast cancer. Cancer Cell 37: 496-513, 2020.
6. Kazi M, Alqahtani A, Alharbi M, Ahmad A, Hussain MD, Alothaid H and Aldughaim MS: The development and optimization of lipid-based self-nanoemulsifying drug delivery systems for the intravenous delivery of propofol. Molecules 28: 1492, 2023.
7. Sun P, Huang H, Ma JC, Feng B, Zhang Y, Qin G, Zeng W and Cui ZK: Repurposing propofol for breast cancer therapy through promoting apoptosis and arresting cell cycle. Oncol Rep 52: 155, 2024.
8. Zhang Y, Yu P, Bian L, Huang W, Li N and Ye F: Survival benefits of propofol-based versus inhalational anesthesia in non-metastatic breast cancer patients: a comprehensive meta-analysis. Sci Rep 14: 16354, 2024.
9. Tian D, Tian M, Ma ZM, Zhang LL, Cui YF and Li JL: Anesthetic propofol epigenetically regulates breast cancer trastuzumab resistance through IL-6/miR-149-5p axis. Sci Rep 10: 8858, 2020.
10. Müller MR, Burmeister A, Skowron MA, Stephan A, Bremmer F, Wakileh GA, Petzsch P, Köhrer K, Albers P and Nettersheim D: Therapeutical interference with the epigenetic landscape of germ cell tumors: A comparative drug study and new mechanistical insights. Clin Epigenetics 14: 5, 2022.
11. Moon S, Kim HJ, Lee Y, Lee YJ, Jung S, Lee JS, Hahn SH, Kim K, Roh JY and Nam S: Oncogenic signaling pathways and hallmarks of cancer in Korean patients with acral melanoma. Comput Biol Med 154: 106602, 2023.
12. Zhang J, Liu F, Guo W, Bi X, Yuan S, Shayiti F, Pan T, Li K and Chen P: Single-cell transcriptome sequencing reveals aberrantly activated inter-tumor cell signaling pathways in the development of clear cell renal cell carcinoma. J Transl Med 22: 37, 2024.
13. Salvati A, Melone V, Sellitto A, Rizzo F, Tarallo R, Nyman TA, Giurato G, Nassa G and Weisz A: Combinatorial targeting of a chromatin complex comprising Dot1L, menin and the tyrosine kinase BAZ1B reveals a new therapeutic vulnerability of endocrine therapy-resistant breast cancer. Breast Cancer Res 24: 52, 2022.
14. Wang S, Bei Y, Tian Q, He J, Wang R, Wang Q, Sun L, Ke J, Xie C and Shen P: PFKFB4 facilitates palbociclib resistance in oestrogen receptor-positive breast cancer by enhancing stemness. Cell Prolif 56: e13337, 2023.
15. Zhu Y, Zhang H, Pan C, He G, Cui X, Yu X, Zhang X, Wu D, Yang J, Wu X, *et al*: Integrated tumor genomic and immune microenvironment analysis identifies predictive biomarkers associated with the efficacy of neoadjuvant therapy for triple-negative breast cancer. Cancer Med 12: 5846-5858, 2023.
16. Li R, Ferdinand JR, Loudon KW, Bowyer GS, Laidlaw S, Muyas F, Mamanova L, Neves JB, Bolt L, Fasouli ES, *et al*: Mapping single-cell transcriptomes in the intra-tumoral and associated territories of kidney cancer. Cancer Cell 40: 1583-1599.e1510, 2022.
17. Shimizu H and Nakayama KI: A 23 gene-based molecular prognostic score precisely predicts overall survival of breast cancer patients. EBioMedicine 46: 150-159, 2019.
18. Xue Y, Lian W, Zhi J, Yang W, Li Q, Guo X, Gao J, Qu H, Lin W, Li Z, *et al*: HDAC5-mediated deacetylation and nuclear localisation of SOX9 is critical for tamoxifen resistance in breast cancer. Br J Cancer 121: 1039-1049, 2019.
19. Lü M, Ding K, Zhang G, Yin M, Yao G, Tian H, Lian J, Liu L, Liang M, Zhu T and Sun F: MicroRNA-320a sensitizes tamoxifen-resistant breast cancer cells to tamoxifen by targeting ARPP-19 and ERRγ. Sci Rep 5: 8735, 2015.
20. Yao J, Deng K, Huang J, Zeng R and Zuo J: Progress in the understanding of the mechanism of tamoxifen resistance in breast cancer. Front Pharmacol 11: 592912, 2020.
21. Leslie EM, Deeley RG and Cole SP: Multidrug resistance proteins: Role of P-glycoprotein, MRP1, MRP2, and BCRP (ABCG2) in tissue defense. Toxicol Appl Pharmacol 204: 216-237, 2005.
22. Liu H, Wang N, Yang R, Luan J, Cao M, Zhai C, Wang S, Wei M, Wang D, Qiao J, *et al*: E3 ubiquitin ligase NEDD4L negatively regulates skin tumorigenesis by inhibiting IL-6/GP130 signaling pathway. J Invest Dermatol 144: 2453-2464.e2411, 2024.
23. Yin R, Gao J and Liu Y: Mechanisms analysis for formononetin counteracted-osimertinib resistance in non-small cell lung cancer cells: From the insight into the gene transcriptional level. Chem Biol Drug Des 103: e14435, 2024.
24. Wang Z, Gerstein M and Snyder M: RNA-Seq: A revolutionary tool for transcriptomics. Nat Rev Genet 10: 57-63, 2009.
25. Angus L, Smid M, Wilting SM, Bos MK, Steeghs N, Konings I, Tjan-Heijnen VCG, van Riel J, van de Wouw AJ, Cpct C, *et al*: Genomic alterations associated with estrogen receptor pathway activity in metastatic breast cancer have a differential impact on downstream ER signaling. Cancers (Basel) 15: 4416, 2023.
26. Sasada S, Kondo N, Hashimoto H, Takahashi Y, Terata K, Kida K, Sagara Y, Ueno T, Anan K, Suto A, *et al*: Prognostic impact of adjuvant endocrine therapy for estrogen receptor-positive and HER2-negative T1a/bN0M0 breast cancer. Breast Cancer Res Treat 202: 473-483, 2023.
27. Barathan M, Vellasamy KM, Ibrahim ZA, Mariappan V, Hoong SM and Vadivelu J: Zerumbone mediates apoptosis and induces secretion of proinflammatory cytokines in breast carcinoma cell culture. Iran J Basic Med Sci 24: 1538-1545, 2021.
28. Icard P, Shulman S, Farhat D, Steyaert JM, Alifano M and Lincet H: How the Warburg effect supports aggressiveness and drug resistance of cancer cells? Drug Resist Updat 38: 1-11, 2018.
29. Kowsari H, Davoodvandi A, Dashti F, Mirazimi SMA, Bahabadi ZR, Aschner M, Sahebkar A, Gilasi HR, Hamblin MR and Mirzaei H: Resveratrol in cancer treatment with a focus on breast cancer. Curr Mol Pharmacol 16: 346-361, 2023.
30. Rasoolnezhad M, Safaralizadeh R, Hosseinpour Feizi MA, Banan-Khojasteh SM, Roshani Asl E, Lotfinejad P and Baradaran B: MiR-138-5p improves the chemosensitivity of MDA-MB-231 breast cancer cell line to paclitaxel. Mol Biol Rep 50: 8407-8420, 2023.
31. Sun C, Liu P, Pei L, Zhao M and Huang Y: Propofol inhibits proliferation and augments the anti-tumor effect of doxorubicin and paclitaxel partly through promoting ferroptosis in triple-negative breast cancer cells. Front Oncol 12: 837974, 2022.
32. Wang H, Zhao L, Wu J, Hong J and Wang S: Propofol induces ROS-mediated intrinsic apoptosis and migration in triple-negative breast cancer cells. Oncol Lett 20: 810-816, 2020.
33. Zhang X, Li F, Zheng Y, Wang X, Wang K, Yu Y and Zhao H: Propofol reduced mammosphere formation of breast cancer stem cells via pd-l1/nanog in vitro. Oxid Med Cell Longev 2019: 9078209, 2019.
34. Malekmohammadi M, Price CM, Hudson AE, DiCesare JAT and Pouratian N: Propofol-induced loss of consciousness is associated with a decrease in thalamocortical connectivity in humans. Brain 142: 2288-2302, 2019.
35. Wakai A, Blackburn C, McCabe A, Reece E, O'Connor G, Glasheen J, Staunton P, Cronin J, Sampson C, McCoy SC, *et al*: The use of propofol for procedural sedation in emergency departments. Cochrane Database Syst Rev 2015: CD007399, 2015.
36. Yoon S, Jung SY, Kim MS, Yoon D, Cho Y and Jeon Y: Impact of propofol-based total intravenous anesthesia versus inhalation anesthesia on long-term survival after cancer surgery in a nationwide cohort. Ann Surg 278: 1024-1031, 2023.
37. Faienza F, Polverino F, Rajendraprasad G, Milletti G, Hu Z, Colella B, Gargano D, Strappazzon F, Rizza S, Vistesen MV, *et al*: AMBRA1 phosphorylation by CDK1 and PLK1 regulates mitotic spindle orientation. Cell Mol Life Sci 80: 251, 2023.

38. Milletti G, Colicchia V and Cecconi F: Cyclers' kinases in cell division: From molecules to cancer therapy. Cell Death Differ 30: 2035-2052, 2023.
39. Decker T, Lüdtke-Heckenkamp K, Melnichuk L, Hirmas N, Lübbe K, Zahn MO, Schmidt M, Denkert C, Lorenz R, Müller V, *et al*: Anti-hormonal maintenance treatment with the CDK4/6 inhibitor ribociclib after 1st line chemotherapy in hormone receptor positive / HER2 negative metastatic breast cancer: A phase II trial (AMICA). Breast 72: 103575, 2023.
40. Ergun Y, Dogan M, Ucar G, Karacin P and Karacin C: Efficacy of adjuvant CDK4/6 inhibitors in hormone receptor-positive breast cancer: A systematic review and meta-analysis. Expert Opin Pharmacother 24: 1901-1909, 2023.
41. Li Q, Jiang B, Guo J, Shao H, Del Priore IS, Chang Q, Kudo R, Li Z, Razavi P, Liu B, *et al*: INK4 tumor suppressor proteins mediate resistance to CDK4/6 kinase inhibitors. Cancer Discov 12: 356-371, 2022.
42. Pandey K, An HJ, Kim SK, Lee SA, Kim S, Lim SM, Kim GM, Sohn J and Moon YW: Molecular mechanisms of resistance to CDK4/6 inhibitors in breast cancer: A review. Int J Cancer 145: 1179-1188, 2019.
43. Paternot S, Bockstaele L, Bisteau X, Kooken H, Coulonval K and Roger PP: Rb inactivation in cell cycle and cancer: The puzzle of highly regulated activating phosphorylation of CDK4 versus constitutively active CDK-activating kinase. Cell Cycle 9: 689-699, 2010.
44. Herrera-Abreu MT, Palafox M, Asghar U, Rivas MA, Cutts RJ, Garcia-Murillas I, Pearson A, Guzman M, Rodriguez O, Grueso J, *et al*: Early adaptation and acquired resistance to CDK4/6 inhibition in estrogen receptor-positive breast cancer. Cancer Res 76: 2301-2013, 2016.
45. Mihály Z, Kormos M, Lánczky A, Dank M, Budczies J, Szász MA and Győrffy B: A meta-analysis of gene expression-based biomarkers predicting outcome after tamoxifen treatment in breast cancer. Breast Cancer Res Treat 140: 219-232, 2013.
46. Wu X, Sun A, Yu W, Hong C and Liu Z: CXCL10 mediates breast cancer tamoxifen resistance and promotes estrogen-dependent and independent proliferation. Mol Cell Endocrinol 512: 110866, 2020.
47. Cao Z, Jin Z, Zeng L, He H, Chen Q, Zou Q, Ouyang D, Luo N, Zhang Y, Yuan Y and Yi W: Prognostic and tumor-immune infiltration cell signatures in tamoxifen-resistant breast cancers. Gland Surg 10: 2766-2779, 2021.
48. Gonçalves TL, de Araújo LP and Pereira Ferrer V: Tamoxifen as a modulator of CXCL12-CXCR4-CXCR7 chemokine axis: A breast cancer and glioblastoma view. Cytokine 170: 156344, 2023.
49. Abdul-Sater AA, Edilova MI, Clouthier DL, Mbanwi A, Kremmer E and Watts TH: The signaling adaptor TRAF1 negatively regulates toll-like receptor signaling and this underlies its role in rheumatic disease. Nat Immunol 18: 26-35, 2017.
50. Lee HJ, Lee JJ, Song IH, Park IA, Kang J, Yu JH, Ahn JH and Gong G: Prognostic and predictive value of NanoString-based immune-related gene signatures in a neoadjuvant setting of triple-negative breast cancer: Relationship to tumor-infiltrating lymphocytes. Breast Cancer Res Treat 151: 619-627, 2015.
51. Weng L, Ziliak D, Lacroix B, Geeleher P and Huang RS: Integrative 'omic' analysis for tamoxifen sensitivity through cell based models. PLoS One 9: e93420, 2014.
52. Jiang C, Zhu Y, Chen H, Lin J, Xie R, Li W, Xue J, Chen L, Chen X and Xu S: Targeting c-Jun inhibits fatty acid oxidation to overcome tamoxifen resistance in estrogen receptor-positive breast cancer. Cell Death Dis 14: 653, 2023.